ELSEVIER

Thermochimica Acta 244 (1994) 153–169

thermochimica acta

Determination of polymeric sulfur stability by differential scanning calorimetry ☆

J.M. Jiménez-Mateos, C. Rial*, F. Temprano

REPSOL, Centro de Investigación, C/ Embajadores 183, 28045 Madrid, Spain

Received 15 November 1993; accepted 19 January 1994

Abstract

The stability of industrial polymeric sulfur is a key parameter in the characterization of this material. In the present work, a method based on differential scanning calorimetry (DSC) for the determination of the stability of polymeric sulfur is proposed as an alternative to the gravimetric "classical" method. This calorimetric method is simple and allows estimation of the stability in a short time and with adequate precision, and is thus suitable for plant control purposes.

Keywords: DSC; Stability; Sulphur

1. List of symbols

a	Intercept of regression curve
ANOVA	Analysis of variance
b	Slope of regression curve
CV	Coefficient of variation (s_e/b)
df	Degrees of freedom
DSC	Differential scanning calorimetry
F	Statistic used to compare variances
H	Integrated value (J g^{-1}) of a DSC effect

☆ Presented in part at the Latin-American Inorganic Chemistry Meeting, held at Santiago de Compostela, Spain, September 1993.

* Corresponding author.

SSDI 0040-6031(00)01747-5

H_{endo}	H for first endotherm, between 90°C and exothermic
H_{exo}	H for exotherm
$H + H$	Sum of absolute values of H_{endo} and H_{exo}
H_0	Null hypothesis
H_1	Alternative hypothesis
j	Number of sets
MS	Mean square (SS/df)
N	Total number of values
n_j	Number of values corresponding to set j
r	Correlation coefficient
$S(\%)$	Stability of polymeric sulfur (as defined in Ref. [3])
SS	Sum of squares
s^2	Variance
s	Standard deviation (experimentally determined)
s_b	Experimental standard deviation due to different analysts and to inherent errors of the method
s_c	Experimental standard deviation between all groups of samples
s_e	Total experimental standard deviation of the regression
s_l	Experimental standard deviation of the regression due to lack of fit
s_p	Experimental standard deviation of the regression due to pure error
$(se)_x$	Standard error of x ($s/\sqrt{n}$)
t	Student's statistic used in comparing two averages
X	Independent variable in regression ($S(\%)$)
x	Value of an observation
$\bar{x}$	Arithmetic average of values of x
Y	Dependent variable in regression (H_{endo}, H_{exo}, $H + H$, $H - H$)

1.1. Greek letters

α	Level of significance or confidence level
μ	Population average or mean
σ	Population standard deviation

2. Introduction

Elemental sulfur undergoes reversible polymerization on heating to temperatures above 159°C [1]. Polymeric sulfur presents a wide range of potential applications [2]. Many attempts to stabilize this form of sulfur by various additives inhibiting the depolymerization (which occurs below 159°C) have been carried out. However, most of these modified sulfurs studied so far harden or recrystallize to more stable phases. The stability of polymeric sulfur is then a critical parameter to take into account in the production process of this metastable material.

The sulfur manufacturer Crystex [3] defines the stability $S(\%)$ of polymeric sulfur as the fraction of insoluble sulfur remaining in the sample (determined by extrac-

tion with CS_2) after heat treatment in tetralin at 110°C for 15 min. This "classical" method, although widely used, is rather laborious.

Differential scanning calorimetry (DSC) provides information about the evolution of a material versus temperature and/or time, and is a valuable tool for studying endothermic and exothermic processes. DSC also allows the determination of the reaction enthalpies by peak area integration. This technique has been applied previously in the characterization of sulfur [4–10]. As the stability is a characteristic property of metastable polymeric sulfur, there should exist a parameter, obtainable from the thermogram, relating the evolution of the polymer to temperature and to its stability calculated by the classical method. This parameter has been determined, and a new method for estimating the stability of polymeric sulfur by applying DSC is proposed. The results obtained are precise enough for the purpose of plant control, and the DSC method is easier to perform. It should be stressed that the aim of this work is not to interpret the thermograms correctly but to develop an analytical method which can be used for routine plant control.

3. Experimental

Industrial polymeric sulfur samples obtained in a pilot plant by quenching liquid or vapor sulfur were used for this study. Their stabilities versus temperature were determined by the classical method [3] depicted in Fig. 1.

The DSC measurements were carried out on a Perkin-Elmer DSC-7 calorimeter equipped with a robotic system and a standard cell. Measurements were run on ≈ 7 mg polymeric sulfur samples in aluminum capsules (40 µl vol., 0.15 mm thick, $P_{max} = 2$ bar) under the following experimental conditions: temperature range 30–200°C, scan rate 5°C min^{-1}, nitrogen purge gas flow rate 25 ml min^{-1}. These conditions provided both good resolution and sensitivity, as was confirmed by running experiments at different scanning rates (see Fig. 2a). Upper and lower temperature limits were chosen to be far enough from the effects in order to obtain a stable baseline.

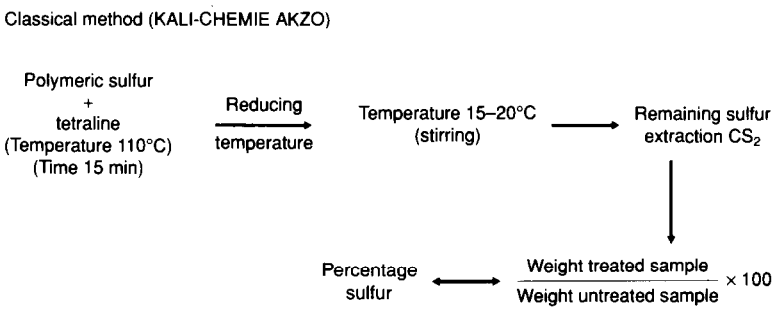

Fig. 1. Scheme of the classical gravimetric method.

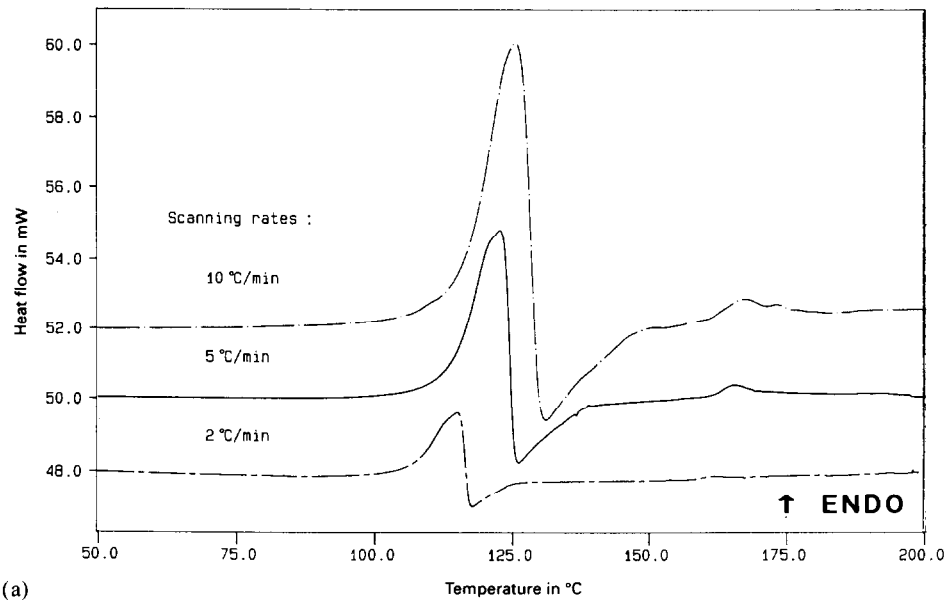

(a)

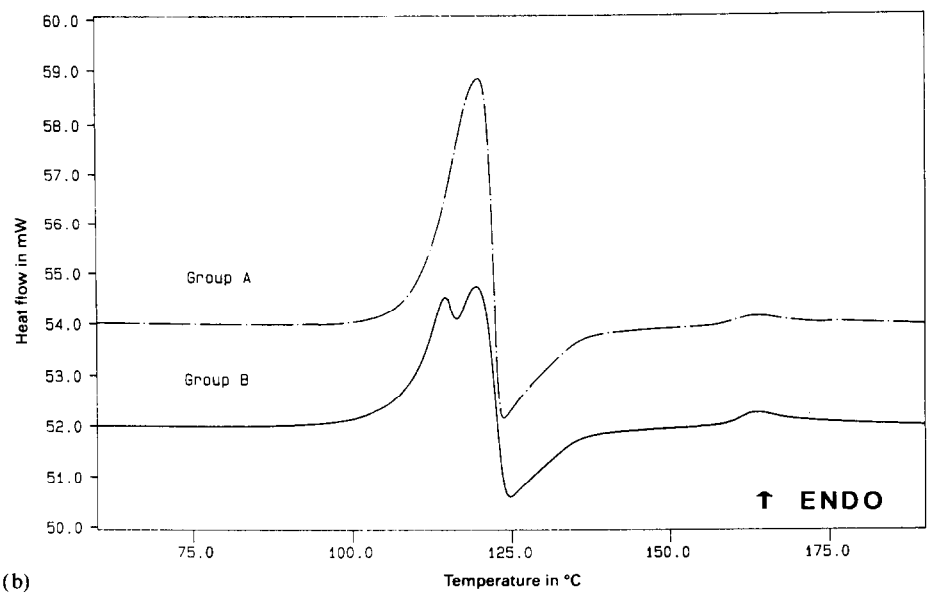

(b)

Fig. 2. Typical DSC thermograms of polymeric sulfur: (a) using different scanning rates (10, 5 and 2°C min^{-1}); (b) showing a single (Group A) and a double (Group B) endothermic effect.

Data treatment was performed with the Perkin-Elmer 7 Series UNIX/DSC Software [11]. Statistical analysis of the data was carried out using the program STATGRAPHICS [12].

4. Results

DSC experiments were performed on insoluble sulfur samples with different stabilities, which were previously standardized by the classical method. It should be noted that, as these samples will be used as standards, the determination of their classical stabilities was carried out rigorously.

All thermograms obtained in the temperature range 30–200°C show two characteristic effects (Fig. 2(b)):

1. In the temperature range 90–140°C, a complex effect is observed in which at least two transitions are involved. The first, a strong endothermic effect, is due to the melting of the polymer and the rupture of the chains [7]. It is followed immediately by an exothermic effect, which corresponds to the reversion of the metastable melt to S_8 molecules [7].

2. Around 160–170°C an endothermic effect due to polymerization of the liquid is observed.

Regarding the first effect, occurring between 90 and 140°C, the endotherm can be single or double (Fig. 2(b)). It should be pointed out that no satisfactory explanation of this observation has so far been found. The double effect could be due to the presence of at least two different well defined polymeric chain length distributions ("phases") in the samples, thus giving rise to two separate effects corresponding to different melting stages. The correct interpretation of these results is outside the scope of this work, our goal being simply to establish an analytical procedure. Nevertheless, further work is in progress. The studied polymeric sulfur samples can be classified into two groups, depending on whether the thermograms show a simple (Group A) or a double endotherm (Group B).

It is clear that these effects observed in the temperature range 90–140°C cannot be considered as being due to simple transitions (melting or reversion), but rather as the result of the overlap of several transitions of the different phases involved in the material (polymeric sulfur, S_8, etc.) which take place simultaneously or consecutively. This difficulty in separating the different effects on the thermograms renders their individual integration impossible, and the obtained integrated energies would not correspond to simple transitions.

In order to establish a systematic method for obtaining comparable energetic parameters (i.e. characteristic "energies") from all thermograms, two temperature intervals between precisely defined points on the thermograms have been chosen for carrying out the integrations. It is worth noting that these integrations are calculated with sigmoidal baselines to improve the reproducibility in the integration of the peaks, and thus to avoid errors arising from the choice of the integration limits. When the calculations are performed with linear baselines the integrated data are poorly reproducible (Fig. 3). It should be mentioned that the choice of this type of baseline is based on analytical criteria (reproducibility and repeatability), as a sigmoidal baseline has limited physical meaning in these experiments.

The first integration interval is taken from 60°C to the temperature at the bottom of the exothermic effect (reversion to S_8 molecules). The integrated area corresponding to this interval will be called $H_{endo}/(J\ g^{-1})$. The second integration

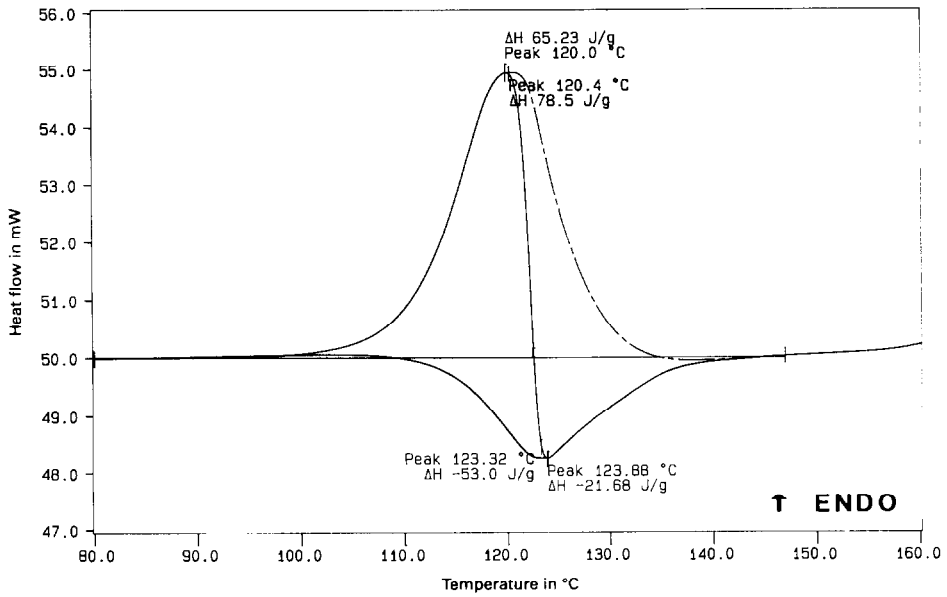

Fig. 3. Determination of the "energetic" integrated parameters H_{endo} and $H_{exo}/(J\ g^{-1})$ by peak area integration using both linear and sigmoidal baselines.

interval is defined between the temperature corresponding to the top of the endothermic effect associated with the melting of the polymer and the inflexion point in the baseline indicating the beginning of the endothermic effect associated with polymerization. The resulting integrated area will be called $H_{exo}/(J\ g^{-1})$.

The parameters H_{endo} and H_{exo} do not correspond to energies associated with simple transitions. However, calculations have been carried out over equivalent regions on all thermograms, so it can be assumed that the obtained integrated "energies" represent equivalent processes occurring in the samples.

Thus, from DSC thermograms of polymeric sulfur samples previously standardized by the classical method, two characteristic energetic parameters are obtained, namely H_{endo} and H_{exo}. Calibration patterns have been drawn that display these energetic parameters for each sample versus the corresponding stability. By referring to these curves the values of H_{endo} and H_{exo} for a sample of unknown stability, the stability of the sample can be determined.

The classical method yields values of $S(\%)$ which correspond to the ratio of the weight of the polymeric sulfur sample before and after extraction with CS_2. These materials are often modified with stabilizers and other additives not accounted for when weighing the sample, thus introducing a systematic error in the determination of the stability of the sample. The control of temperature is also very important for obtaining reproducible results. To prove this point, two sets of determinations of $S(\%)$ for a polymeric sulfur sample at two different temperatures have been performed. The results are shown in Table 1. To test the variances, the F test ($\alpha = 0.05$, two-tailed) has been performed:

Table 1
Two sets of determinations of $S(\%)$ for a polymeric sulfur sample at two different but close temperatures, using the classical method. Mean stability values and standard deviations for both sets and pooled values are included

	$S(\%)$	$\bar{S}(\%)$	s
Set I; $T = 104.5°C$	77.8 79.3 78.2	78.4	0.78
Set II; $T = 105.0°C$	74.9 74.6 73.5 75.5 76.0	74.9	0.95
pooled values		76.7	1.99

$$H_0: \sigma_I^2 = \sigma_{II}^2 \quad H_1: \sigma_I^2 \neq \sigma_{II}^2 \tag{1}$$

giving $F = 0.67$ and $F_{0.05/2,2,4} = 10.6$. We can accept the null hypothesis H_0 and conclude that the variances are equal at $\alpha = 0.05$.

To test the averages, a two-tailed t test is carried out:

$$H_0: \mu_I = \mu_{II} \quad H_1: \mu_I \neq \mu_{II} \tag{2}$$

giving $t = 5.39$ (df = 6) and $t_{0.05/2,6} = 2.45$. Here, the critical t value is exceeded, and we can thus conclude that there is a significant difference between the averages at $\alpha = 0.05$.

According to these results it is worth noting the critical influence of temperature in the determination of the stability by the classical method. The precise control of this parameter is necessary if these $S(\%)$ values are to be considered as constants, as is the case in the standardization of samples for the development of the new method described below. On the other hand, as the treatment temperature is a critical parameter in this method, routine measurements are often affected by a significant error ($\sigma \geqslant 2\%$) arising from insufficiently strict control of this factor or, indeed, from such inherent properties as the low thermal conductivity of sulfur.

Table 2
Polymeric sulfur samples standardized by the classical method. Classical stability values $S(\%)$ and number of replicate measurements by DSC n_j are included. Samples are classified into Group A and Group B, depending on the number of endotherms (see text)

Group A		Group B	
$S(\%)$	n_j	$S(\%)$	n_j
63.9	8	31.0	5
64.9	6	39.0	6
66.6	6	50.0	6
67.1	4	55.0	3
70.9	9	65.0	6
71.6	4	69.0	9
71.9	6	73.5	3
72.1	6		
72.9	5		
75.3	8		

For our study, two series of polymeric sulfur samples showing different features in their DSC behaviour have been investigated. Table 2 shows these two groups of samples (Group A and Group B) and their respective classical stability sets. No universal calibration pattern could be constructed, but two different calibration curves were obtained, each suitable for a group of samples having the same thermal behaviour.

In order to estimate $S(\%)$ for a sample from its known H_{endo} and H_{exo} values, we have studied the possible relationships between these parameters and the stability determined by the classical method. The best calibration curves for Group A and Group B were calculated. Statistical calculations were performed according to the methodology of Ref. [13], using the program STATGRAPHICS [12].

5. Statistical analysis

5.1. Preliminary statistical study

The detailed statistical analysis for Group A will be described. Equivalent results, not included here, were obtained for Group B. The variable yielding good correlation with $S(\%)$ and the best calibration graphs must be established. H_{endo}, H_{exo} and the linear combinations $|H_{endo}| + |H_{exo}|(H + H)$ and $|H_{endo}| - |H_{exo}|(H - H)$ are proposed as variables. An analysis of variance (ANOVA; see Table 3) for each variable is performed to confirm whether any real differences exist between their values for each stability set. The confidence level considered will be set at $\alpha = 0.05$ from this point. For this analysis, the variance (MS) between sets is greater than that within sets, confirming that there exists a variation of all variables with $S(\%)$ for the accepted confidence level. However, the degree of variation is not the

Table 3
ANOVA for sets of samples corresponding to Group A

Variable	Source	SS	df	MS	F [a]
H_{endo}	between sets	294.91025	9	32.767805	163.683
	within sets	10.40992	52	0.200191	
	total	305.32017	61		
H_{exo}	between sets	843.28472	9	93.698302	251.485
	within sets	19.0016	51	0.372580	
	total	862.28632	60		
$H + H$	between sets	2101.8497	9	233.53886	314.073
	within sets	37.9226	51	0.74358	
	total	2139.7724	60		
$H - H$	between sets	175.00094	9	19.444549	48.577
	within sets	20.41443	51	0.400283	
	total	195.41536	60		

[a] $F_{0.05,9,51} = 2.065$.

Table 4
Bartlett's test: homogeneity of variances between sets for the studied variables

Variable	df_1	df_2	F	$F_{0.05,9,df2}$
H_{endo}	9	1084	1.38604	1.880
H_{exo}	9	1722	1.23183	1.885
$H+H$	9	1722	1.23378	1.885
$H-H$	9	1722	1.21025	1.885

same for each variable, and that providing the best sensitivity and reproducibility must be chosen.

By using the Bartlett test, the homogeneity of variances between the different groups has been proved (Table 4). It is then possible to estimate the pooled variances for each variable (s_p^2). Table 5 gives the corresponding standard deviations s_p, together with the standard deviation due to variability among the sets.

In Fig. 4, the average values for H_{endo}, H_{exo}, $(H+H)$ and $(H-H)$ calculated for each stability set and their 95% confidence intervals are represented. The only clear conclusion to be drawn from this plot is that $H+H$ appears to yield the best sensitivity.

To decide which variable gives the best calibration curve, two criteria based on s_p and s_c (Table 5) are applied:

1. From the comparison of the corresponding s_p values, the variables can be ordered according to the error in their determination: $H_{endo} < H_{exo} < H-H < H+H$;

2. Comparing the s_c values, the variable providing the best sensitivity for the calibration curve will be that with higher s_c; thus the following order, from the highest to the lowest sensitivity, can be established: $H+H > H_{exo} > H_{endo} > H-H$.

Unfortunately these criteria lead to conflicting conclusions, and only $H-H$ can be clearly rejected. Thus the calibration curves for the rest of the variables must be calculated in order to select the most appropriate.

Before considering which variable might be the best for drawing our calibration graph, it would be convenient to study the reproducibility and repeatability of the

Table 5
Pooled standard deviation for each variable s_p and standard deviation for each variable due to variability between sets s_c

Variable	s_p	n'	s_c
H_{endo}	0.447427	6.1541219	2.3004348
H_{exo}	0.6103933	6.0510018	3.9272363
$H+H$	0.8623108	6.0510018	6.2025953
$H-H$	0.6326792	6.0510018	1.7740607

$s_c^2 = (SS_c/(j-1) - s_p)/n'$
$n' = (N^2 - \Sigma n_i^2)/(j-1)N$

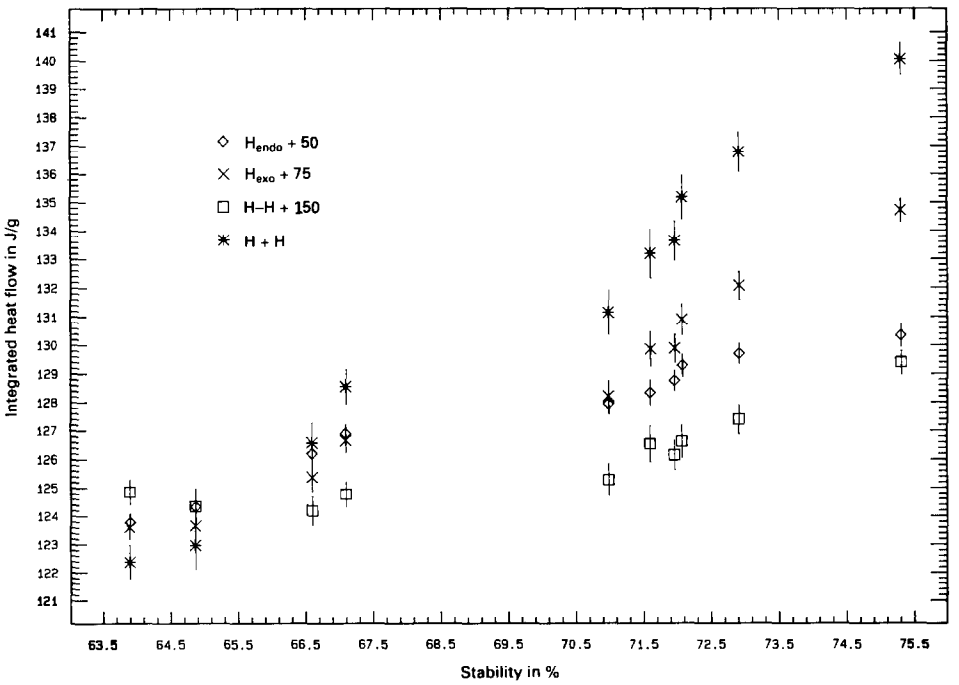

Fig. 4. Average values and confidence intervals ($\alpha = 0.05$, vertical bars) for H_{endo}, H_{exo}, $H + H$ and $H - H$/(J g^{-1}) versus standardized classical stability, S(%), corresponding to Group A. Note that the scales for H_{endo}, H_{exo} and $H - H$ are shifted by 50, 75 and 150 J g^{-1}, respectively.

determination for the remaining variables H_{endo}, H_{exo} and $H + H$. For this purpose, a test involving four sets of samples and two analysts was performed and the results were treated by ANOVA. This ANOVA and the intermediate results are not included here but are available from the authors. From the findings, it was concluded that the main source of error in this method is the determination of H_{endo} and H_{exo} from the thermograms; the factors involved in running the experiments are then not so critical. On the other hand, the differences between analysts were much lower than those for the measurements within a set. Considering $\mu = \bar{x} + 2.775s^2$ (Ref. [13], pp. 84 and 135) and using s_p (Table 5) for repeatability and $(s_b)_p$ (pooled s_b values, see Table 6, resulting from ANOVA of Ref. [13], p. 135) for reproducibility, the final values of the corresponding results are displayed in Table 6.

5.2. Regression analysis

Once the repeatability and the reproducibility have been considered, the regression equations fitting the experimental results are determined in order to select the variable providing the best calibration curve. Various models have been tested:

Table 6
Pooled standard deviation due to different analysts and intrinsic errors of the method [$(s_b)_p$, with df = 34], repeatability and reproducibility for the determination of the variables

Variable/(J g^{-1})	$(s_b)_p$	Repeatability	Reproducibility
H_{endo}	0.4607577	±1.24 (1.6%)	±1.39 (1.8%)
H_{exo}	0.7151595	±1.69 (3.2%)	±2.27 (4.2%)
$H + H$	0.9319809	±2.39 (1.8%)	±2.66 (2.0%)

linear ($Y = a + bX$), exponential [$Y = \exp(a + bX)$], potential ($Y = aX^b$), and inverse ($1/Y = a + bX$, $Y = a + b/X$), where Y/(J g^{-1}) is the dependent variable (H_{endo}, H_{exo}, $H + H$) and X is the independent variable [S(%)]. The values of X have been treated as constants to simplify the calculations because they are supposed to be accurately known, or at least the error associated with their values is much less than that associated with the Y values [13]. However, this assumption is not really valid, because the determination of the stability of the samples by the classical method, although performed carefully, involves substantial errors, as can be seen from Table 1. For this reason it is very important to determine S(%) rigorously for samples to be considered as standards. Table 7 shows the correlation coefficients r for these fittings. The variation of correlation coefficients between the different models for a given variable is negligible, and the simple linear model has been chosen to fit all three variables.

As has been mentioned before, the samples studied have been classified into two groups, A and B, according to their thermal behaviour. Therefore two separate regression analyses were carried out.

The linear model $Y = a + bX$ [Y/(J g^{-1}) = H_{endo}, H_{exo}, $H + H$; $X = S$(%)] is applied to fit the experimental data, and the results of the different regressions are compared in order to decide which calibration curve provides the best fit.

Table 8 shows the calculated a and b parameters together with the confidence limits ($\alpha = 0.05$) and the standard errors of the correlation coefficients for Groups A and B. The corresponding analyses of variance are shown in Table 9. Fig. 5 shows the linear fittings for each variable, including confidence and prediction limits, together with the corresponding residuals plots for Groups A and B.

Table 7
Correlation coefficients for least squares regressions corresponding to different models for Group A [$X = S$(%)]

Y/(J g^{-1})	$Y = a + bX$	$Y = \exp(a + bX)$	$Y = aX^b$	$1/Y = a + bX$	$Y = a + b/X$
H_{endo}	0.960822	0.959374	0.962180	−0.957748	−0.965496
H_{exo}	0.970701	0.973949	0.971766	−0.976116	−0.964625
$H + H$	0.979541	0.979959	0.979606	−0.979829	−0.977554

Table 8
Intercept a and slope b corresponding to the least squares regressions $Y/(J\ g^{-1}) = a + bS(\%)$ (Y: H_{endo}, H_{exo} and $H + H$). Confidence intervals ($\alpha = 0.05$), standard errors se_a and se_b for the intercept and the slope, respectively, and correlation coefficients r are included

Y	a	se_a	b	se_b	r
Group A					
H_{endo}	38.55550 ± 2.91290	1.455900	0.559380 ± 0.0416810	0.0208318	0.960822
H_{exo}	-12.65550 ± 4.28050	2.140240	0.950491 ± 0.0612632	0.0306316	0.970711
$H + H$	25.83920 ± 5.64732	2.823660	1.519020 ± 0.0808258	0.0404129	0.979541
Group B					
H_{endo}	51.13420 ± 1.07580	0.537877	0.3845310 ± 0.018954	0.00947683	0.989243
H_{exo}	19.40160 ± 0.82230	0.411139	0.3736550 ± 0.014930	0.00746485	0.994263
$H + H$	70.01540 ± 1.09080	0.545379	0.7637020 ± 0.019804	0.00990217	0.997571

6. Discussion

Through the comparison of variances (MS) due to the model and to the total error (which includes the variation not accounted for in the model) for every variable using the F test, the hypothesis that there exists a linear relationship between the variables and $S(\%)$ is accepted ($\alpha = 0.05$; Table 9).

For every $S(\%)$ value, replicate measurements were made of the variables. It was then possible to break down the total error s_e^2 into two terms [13]: pure error s_p^2 and error due to the lack of fit s_l^2. The pure error is the intrinsic error of the experimental system s_p^2. The lack of fit error s_l^2 stems from the divergence from the proposed linear model and is used to decide whether the model is appropriate or whether another model is needed to describe the relationship. The value of the error due to the lack of fit must not exceed that of the pure error. To test this point, the mean squares for lack of fit and for pure error are compared via the F test, being the null hypothesis H_0: $\sigma_p^2 = \sigma_l^2$.

Carrying out this test for our data, the following results have been obtained.

Group A

In every case the value of F ($\alpha = 0.05$) exceeds the critical value; thus the null hypothesis is rejected and the alternative hypothesis H_1: $s_p^2 < s_l^2$ is accepted (Table 9). According to these results, the linear model does not fit the data. However, the adoption of other models does not improve the result (Table 7), which is $s_p^2 < s_l^2$ for each of them. On the other hand, in the residuals plots corresponding to the linear fittings (Fig. 5) no clear trend is observed, the residuals being randomly distributed. Thus, it is suspected that the error due to the lack of fit arises not only from the misfit but from other problems. In fact, the values of the stability $S(\%)$ determined by the classical method have been assumed to be constant when calculating the regression curves, and their determination has been considered as being free from errors. As has been seen before, these assumptions are not strictly true. However,

Table 9
ANOVA for regression $Y/(J\ g^{-1}) = a + bS(\%)$, groups A and B

Variable	Source	SS	df	MS	F
Group A					
H_{endo}	model	281.86530	1	281.86530	721.04
	total error	23.454865	60	0.3909140	
	lack of fit	13.044937	8	1.6306171	8.15
	pure error	10.409928	52	0.2001909	
	TOTAL	305.32017	61		
H_{exo}	model	812.49889	1	812.49889	962.84
	total error	49.787431	59	0.8438550	
	lack of fit	30.785871	8	3.8482338	10.32
	pure error	19.001560	51	0.3725796	
	TOTAL	862.28632	60		
$H + H$	model	2053.1124	1	2053.1124	1397.81
	total error	86.659919	59	1.468812	
	lack of fit	48.737343	8	6.0921679	8.19
	pure error	37.922576	51	0.74345799	
	TOTAL	2139.7724	60		
$F_{0.05,1,60} = 4$	$F_{0.05,1,59} = 4$	$F_{0.05,8,52} = 2.12$	$F_{0.05,8,51} = 2.13$		
Group B					
H_{endo}	model	1176.4414	1	1176.4414	1646.41
	total error	25.723810	36	0.7145500	
	lack of fit	12.764396	5	2.5528792	6.11
	pure error	12.959414	31	0.4180456	
	TOTAL	1202.1652	37		
H_{exo}	model	1008.3994	1	1008.3994	2505.53
	total error	11.671602	29	0.4024690	
	lack of fit	2.6199095	4	0.6549773	1.81
	pure error	9.0516925	25	0.3620677	
	TOTAL	1020.0710	30		
$H + H$	model	4212.4850	1	4212.4850	5948.23
	total error	20.537562	29	0.708192	
	lack of fit	5.3123670	4	1.3280918	2.18
	pure error	15.225195	25	0.6090078	
	TOTAL	4233.0226	30		
$F_{0.05,1,36} = 4.11$	$F_{0.05,1,29} = 4.18$	$F_{0.05,5,31} = 2.52$	$F_{0.05,4,25} = 2.76$		

the aim of this method is to determine $S(\%)$ with errors similar to those incurred in the classical method and, thus, this lack of fit can be tolerated.

Group B

When performing the F test ($\alpha = 0.05$) for H_{endo} (Table 9), the null hypothesis is rejected, which means that H_1: $s_p^2 < s_I^2$ is accepted. On the other hand, for H_{exo} and $H + H$ the null hypothesis H_0: $s_p^2 = s_I^2$ is accepted, with the conclusion that the linear model is not appropriate for fitting the data.

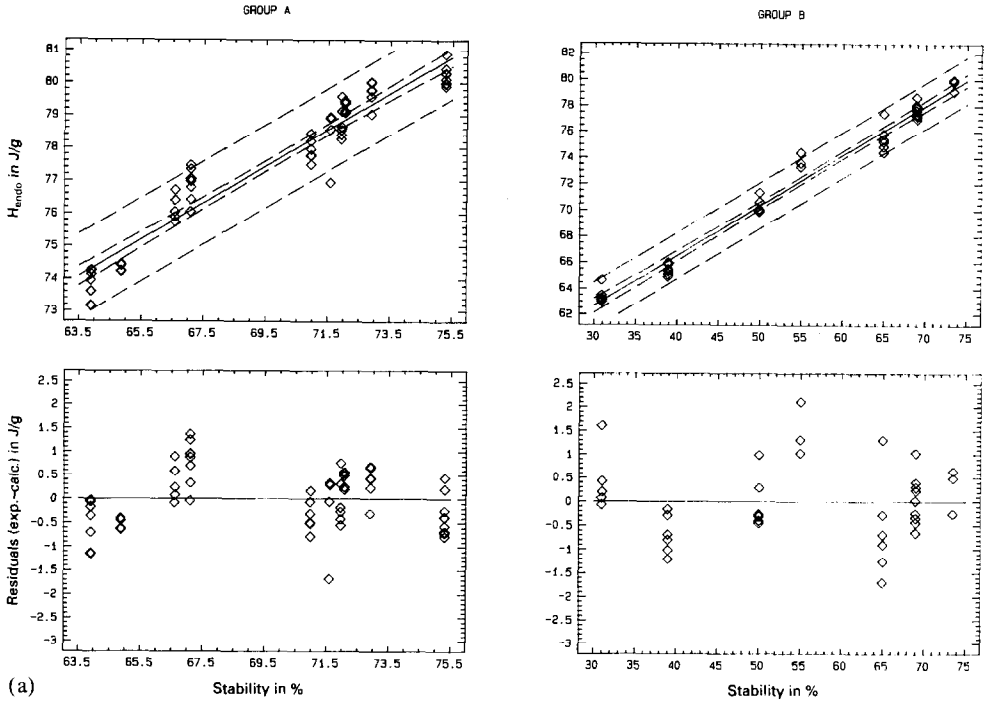
GROUP A
GROUP B
H_{endo} in J/g
Residuals (exp.-calc.) in J/g
Stability in %
(a)

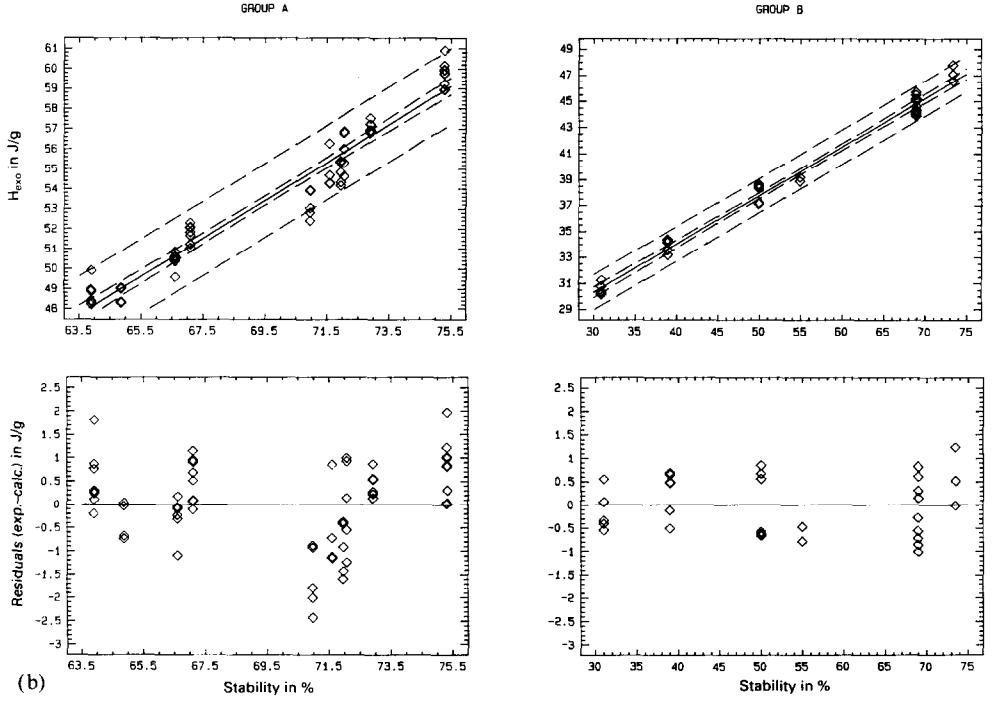
GROUP A
GROUP B
H_{exo} in J/g
Residuals (exp.-calc.) in J/g
Stability in %
(b)

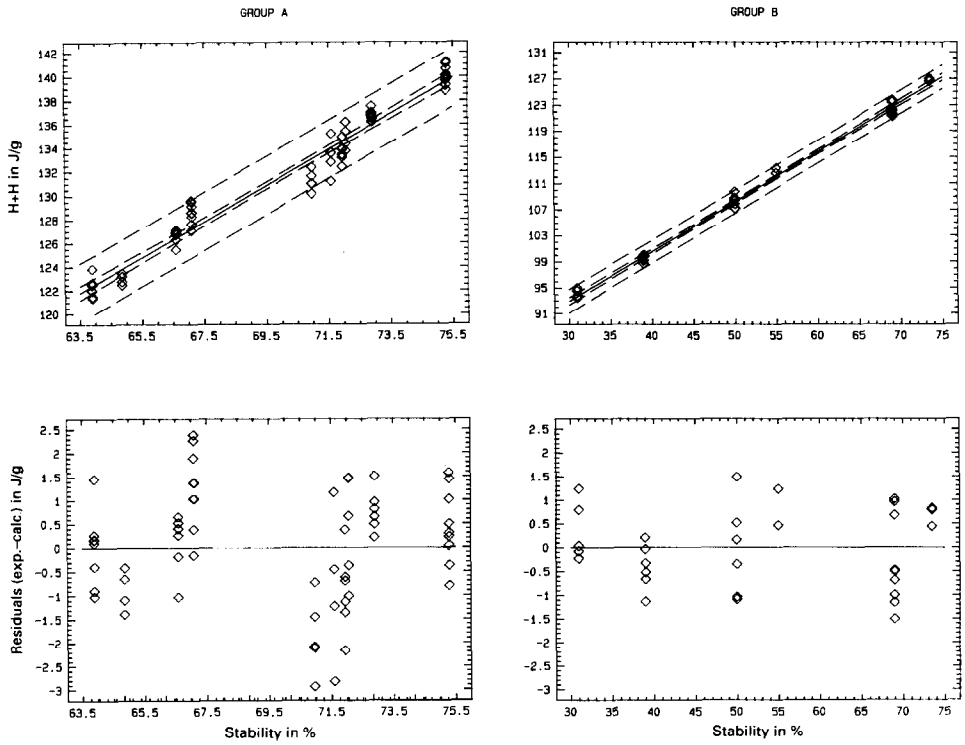

Fig. 5. Least squares regression curves for Groups A and B, corresponding to the linear model $Y = a + bS(\%)$ [$Y/(\mathrm{J\ g^{-1}})$]: (a) H_{endo}; (b) H_{exo}; (c) $H + H$]. Dashed lines correspond to confidence and prediction limits ($\alpha = 0.05$). Residuals plots are also shown.

From the calculated variances of the different errors, the corresponding standard deviations have been determined (Table 10). These parameters, together with the sensitivity (given by the slopes of the calibration curves b in Table 8), should be

Table 10
Standard deviations (total s_e), due to pure error s_p and due to lack of fit corresponding to the least squares regressions $Y/(\mathrm{J\ g^{-1}}) = a + bS(\%)$

Y	s_e	df	s_p	df	s_l	df
Group A						
H_{endo}	0.6252310	60	0.4474269	52	1.2769562	8
H_{exo}	0.9186158	59	0.6103933	51	1.9616916	8
$H + H$	1.2119500	59	0.862318	51	2.4682317	8
Group B						
H_{endo}	0.8435105	36	0.646544	31	1.5977732	5
H_{exo}	0.6344044	29	0.6017206	25	0.8093066	4
$H + H$	0.8415414	29	0.7803895	25	1.1524287	4

Table 11
Coefficients of variation $CV = s_e/b$, groups A and B, for the least squares regressions $Y/(J\ g^{-1}) = a + bS(\%)$

	H_{endo}	H_{exo}	$H + H$
Group A	1.1177	0.9665	0.7978
Group B	2.1983	1.6978	1.1019

used to decide which is the best fit. For our purposes, the best fit will be that providing the lowest errors and the best sensitivity.

Considering the first criterion, the best results for Group A are obtained for H_{endo}, H_{exo} and the worst for $H + H$ (Table 10), and for Group B the best results are given by H_{exo}, $H + H$ and H_{endo} (Table 10), in this order. On the other hand, according to the second criterion, the best fit for Group A is given by $H + H$, followed by H_{exo} and finally H_{endo} (Table 8); for Group B the best fit is given by $H + H$, followed by H_{endo} and H_{exo} (Table 8). In both instances these two criteria again lead to opposing conclusions.

From the above discussion it is clear that, in order to compare the different fittings, a criterion unifying both aspects and indicating unequivocally the calibration curve which provides $S(\%)$ having the lowest errors and the best sensitivity is needed. Therefore a coefficient of variation criterion ($CV = s_e/b$) is proposed. The fit containing the fewest errors and providing the best sensitivity will be that corresponding to the lowest value of CV (Table 11). For both Groups A and B, and according to the values of CV, it is concluded that the most appropriate fit is that involving the variable $H + H$.

The model $H + H/(J\ g^{-1}) = a + bS(\%)$ is therefore chosen to determine $S(\%)$ from the corresponding values of H_{endo} and H_{exo} calculated from the DSC thermograms of the polymeric sulfur samples. Additionally, the error in the estimation of the stability of a problem sample can be computed by using Eqs. (6) and (7) from Ref. [13], p. 102.

Finally, a systematic approach to determining the stability of metastable polymeric sulfur by DSC is proposed. First, a set of samples carefully standardized by the classical method is necessary. This set must cover the full desired range of stability with a sufficient number of samples. DSC thermograms of these samples should be recorded and integrated. From the calculated $H + H$, as before, the calibration curve is computed and used to calculate $S(\%)$ from the thermal data for the problem samples. It should be noted that, once this calibration has been done, further re-calibration will not be necessary, as the accuracy of the data will depend only on the calibration of the calorimeter. It may be prudent to check the system every so often using a standardized sample. Account should be taken of the fact that polymeric sulfur is a metastable phase and thus the stability of a sample will change with time, so that it will be necessary to standardize a control sample just as it is going to be used.

7. Conclusions

A new method has been developed for determining the stability of polymeric sulfur using differential scanning calorimetry. Starting from the stability data determined by the classical method and from the energetic parameters H_{endo} and H_{exo} extracted from the DSC thermograms, both sets of data corresponding to standard polymeric sulfur samples, calibration curves are drawn. The unknown stability value of a sample is thus determined by referring to the calibration curve the energetic parameters obtained from the corresponding DSC thermogram.

Through statistical analysis, the calibration curve providing the best results has been established: $H + H/(\mathrm{J\ g^{-1}}) = a + bS(\%)$. The repeatability and reproducibility ($<2\%$) of the method are acceptable for plant control purposes. Once the calibration curves have been obtained, this method provides a very simple and rapid way of determining the stability of polymeric sulfur samples.

Acknowledgments

The authors thank M. del Mazo and Dr. A. Gonzalo-Aizpiri for their initial work on this subject.

References

[1] W.J. Macknight and A.V. Tobolsky, in B. Meyer (Ed.), Elemental Sulfur, Interscience, New York, 1965, p. 65.
[2] M.D. Barnes, in B. Meyer (Ed.), Elemental Sulfur, Interscience, New York, 1965, p. 357.
[3] Internal Standard, March 1992, Kali-Chemie Akzo.
[4] G.W. Miller, J. Appl. Polym. Sci., 15 (1971) 1985.
[5] B.R. Currell and A.J. Williams, Thermochim. Acta, 9 (1974) 255.
[6] M. Kuballa and G.M. Scheneider, Ber. Bunsenges., 75 (6) (1971) 513.
[7] R. Steudel, S. Passlack-Stephan and G. Holdt, Z. Anorg. Allg. Chem., 517 (1984) 7.
[8] R. Steudel, in A. Mueller and B. Krebs (Eds.), Sulfur: The Significance for Chemistry, Elsevier, Amsterdam, 1984, p. 3.
[9] R. Steudel, Phosphorus Sulfur, 16 (1984) 251.
[10] H. Fisher, in Ullmanns Encyklopädie, Vol. 21, Verlag Chemie, Weinheim, 1982, p. 1.
[11] 7 Series/UNIX, DSC 7 Users Manuals, Perkin-Elmer, Norwalk, CT, 1992.
[12] STATGRAPHICS, Statistical Graphics System, Statistical Graphics Corporation, Version 4.0.
[13] R.L. Anderson, Practical Statistics for Analytical Chemists, Van Nostrand Reinhold, New York, 1987.